ACS AuthorChoice

Environmental Science & Technology

Article

pubs.acs.org/est

Insights into the Composition and Sources of Rural, Urban and Roadside Carbonaceous PM_{10}

Mathew R. Heal* and Mark D. Hammonds

School of Chemistry, The University of Edinburgh, West Mains Road, Edinburgh, EH9 3JJ, United Kingdom

Supporting Information

ABSTRACT: Insights into the nature and sources of the urban and roadside increments in carbonaceous PM_{10} are gained from bulk chemical analyses on daily filter samples collected at a roadside, urban background and rural site in Edinburgh, UK (not all sampling contemporaneous). The concentrations of PM_{10} water-soluble organic matter (WSOM) at the three sites were similar, and (where measured concurrently) strongly correlated, indicating a uniform background source, in contrast to the black carbon component (quantified by filter optical reflectance) whose average concentrations at urban background and roadside were, respectively, about 3 and 7 times greater than at the rural site, indicating local urban sources. BC was not a major component of PM_{10} but was a major component of the urban and roadside PM_{10} increments (~50% and ~60% respectively). The roadside WSOM had greater hydrophobicity than the urban background WSOM. UV−vis spectra indicated increased prevalence of unsaturated bonds and conjugation in urban background WSOM in winter compared with summer. This is consistent with both summertime photochemical production of particle OM and maritime primary aliphatic WSOM. Raman microscopy of a small subset of samples indicated carbon functionality ranged between diesel-like material and more complex humic-like material. Results overall indicate the presence of a background functionalized carbonaceous material, with local BC sources superimposed.

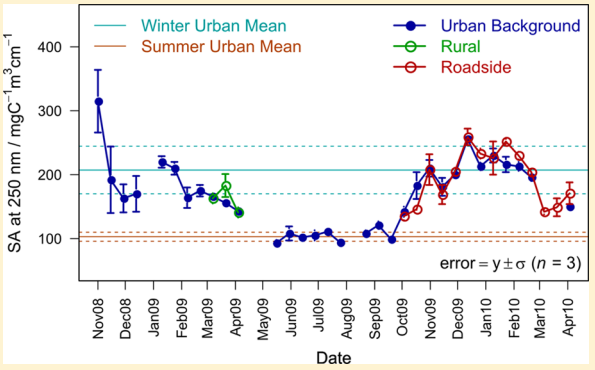

INTRODUCTION

Ambient particulate matter (PM) has a wide range of health and environmental impacts and as a consequence there are considerable drivers to reduce its concentrations.[1] Carbonaceous material constitutes a substantial proportion, at least one-third, of PM composition,[2−7] so knowledge of the components and sources contributing to this component is essential for developing PM mitigation options.

The carbonaceous material of PM is difficult to characterize because it comprises a complex array of chemical components ranging from graphitic elemental carbon to highly functionalized large organic molecules that are hard to separate and identify.[8,9] Nevertheless information on the chemical nature and sources of the carbonaceous material can be derived from parallel application of analytical techniques that provide broader chemical characterization rather than full molecular speciation, and to samples collected from different types of site.

The aim of this work was to apply a combination of carbonaceous analyses to PM samples collected at three different site types—rural, urban background, and roadside—in Edinburgh, UK. The chemical comparison of PM collected at such sites yields valuable insights into the differential contributions of regional background, local urban and traffic sources.[10,11] The traffic sector is an important source of PM which is revealed by the roadside increment.[12−15] This work adds to previous work by examining the roadside increment in aspects of the carbonaceous PM concentrations, whereas previous work predominantly focuses on particle size fractions and/or elemental markers. The optical black carbon (BC) metric has been shown to correlate well with thermal measurements of elemental carbon (EC) mass concentration[16] and to be a reasonable marker for a traffic source of particles.[17] Raman microscopy of individual particles or particle agglomerates has demonstrated utility for determining the extent of the graphitic, that is, soot, nature of particulate carbon.[18−20] Qualitative information on the extent of aromaticity and prevalence of C═C and C═O unsaturated bonds of the water-soluble organic matter (WSOM) component of the PM can be obtained from UV−vis spectroscopy on aqueous extractions.[21] The methodologies described here are applicable to similar studies elsewhere.

MATERIALS AND METHODS

Sampling. Daily (midnight to midnight) samples of PM_{10} were collected by Rupprecht & Pataschnick Inc. Partisol-Plus 2025 samplers (flow rate 16.7 LPM) at an urban background and roadside site in central Edinburgh, UK, and at a rural site

Received: February 19, 2014
Revised: July 12, 2014
Accepted: July 23, 2014
Published: July 23, 2014

   dx.doi.org/10.1021/es500871k | Environ. Sci. Technol. 2014, 48, 8995−9003

Table 1. Urban Background, Rural and Roadside Sampling Site Data and Summary Statistics for the Concentrations of PM_{10}, BC, WSOM, and HWSOM

		urban background			roadside	rural
	lat-long coordinates	3.1821° W, 55.9455° N			3.1823° W, 55.9404° N	3.2058° W, 55.8623° N
	sampling period	20 Aug 2008–21 Apr 2010			10 Sep 2009–21 Apr 2010	25 Feb 2009–21 Apr 2009
		all data	data coincident with roadside	data coincident with rural		
PM_{10}	*n*	576	209	48	209	48
	mean (SD)/$\mu g\ m^{-3}$	15 (8)	15 (8)	18 (12)	18 (9)	14 (10)
	range/$\mu g\ m^{-3}$	1–58	3–48	1–58	3–53	2–42
BC	*n*	576	209	46	209	48
	mean (SD)/$\mu g\ m^{-3}$	1.4 (0.9)	1.6 (1.0)	1.2 (0.7)	3.4 (2.0)	0.5 (0.5)
	range/$\mu g\ m^{-3}$	0.2–6.2	0.2–5.7	0.4–3.0	0.3–11.1	0.1–2.0
WSOM[a]	*n*	491	206	40	206	40
	mean (SD)/$\mu g\ m^{-3}$	1.6 (1.2)	1.7 (1.2)	1.8 (1.5)	1.8 (1.1)	1.6 (1.4)
	range/$\mu g\ m^{-3}$	0.0–10.8	0.0–10.8	0.2–6.3	0.2–6.1	0.2–4.9
HWSOM	*n* (2-week bulk samples)	35	15	3	15	3
	mean (SD)/$\mu g\ m^{-3}$	0.50 (0.18)	0.59 (0.16)	0.61 (0.06)	0.58 (0.18)	0.51 (0.22)
	range/$\mu g\ m^{-3}$	0.11–0.88	0.31–0.85	0.57–0.71	0.29–0.88	0.27–0.71

[a]WSOM data below LOD (22 out of 730 determinations) are retained in the calculations of summary statistics.

~10 km south of the city center. Latitude and longitude coordinates and sample numbers are given in Table 1. Edinburgh is a city of ~450 000 population located near the east coast of Scotland and has relatively low levels of heavy industry and surrounding conurbation. The urban background site was centrally located, but in a small park ~35 m from the nearest main road; samples were collected between 20 August 2008 and 21 April 2010. The roadside location was ~3 m from the kerbside of a busy road (building separation ~19 m and height ~12 m) and ~8 m from a traffic-light controlled intersection with a second busy road; samples were collected between 10 September 2009 and 21 April 2010. The rural site was located in an area of generally agricultural land with the nearest busy road ~500 m away; samples were collected between 25 February 2009 and 21 April 2009. At all sites the sampling inlet was 1.8 m above the ground.

Partisol volumetric flow rates were calibrated every 4 weeks against a NIST traceable critical orifice flow meter from Chinook Engineering. Samples of PM_{10} were collected onto Whatman plc QM-A prebaked (10 h, 500 °C) 47 mm diameter high-purity quartz microfiber filters.

Gravimetric PM_{10}. Filters were weighed in triplicate before and after sample collection on a Sartorius MC5 6-place balance, equipped with antistatic ionizing blower. The two Partisol blank filters (mounted in the Partisol filter cartridge but not exposed) were interspersed in the pre- and postweighing sessions of each batch of sample filters. All filters were conditioned in an undisturbed room for 2 weeks before weighing, and the mean change in blank filter mass between weighing sessions used to correct the sample filter mass changes. Min, 10th percentile, median, 90th percentile and max filter mass corrections were, respectively, −27, 0, 22, 99, and 156 μg. Recorded temperature and relative humidity variation in the conditioning and balance room (19 ± 3 °C and 45 ± 12%) exceeded reference method tolerances[22] but assurance in the correction procedure used here is derived from the high correlation (r = 0.94) and unity gradient between 384 pairs of daily gravimetric and TEOM-FDMS PM_{10} values at the urban background site.

Black Carbon (BC). The optical reflectance, R, of each filter sample was measured with a Diffusion Systems Ltd. EEL MD43 reflectometer. For 513 days within the measurement period at the urban background site values of BC were available from a Magee AE21 Aethalometer operated as part of a UK national network. By consideration of the similarities in the physics of the two measurement methods, a general expression for calculating BC from the reflectance of a Partisol PM_{10} filter was derived as follows. The equation for calculating BC from an Aethalometer when the Virkkula et al.[23] "shadowing" correction is used, is

$$\mathrm{BC}(/\mu g\,m^{-3}) = \frac{A.10^6}{V.\,\alpha_{\mathrm{ATN}}}\ln\left(\frac{I'_0}{I'}\right)\left(1 + k\ln\left(\frac{I_0}{I}\right)\right) \quad (1)$$

where A is the sample area, V is the volume of air sampled, I_0 and I are the light intensity of beams passing through the reference filter and the sample respectively, and k is a shadowing correction applied to each sampling spot on the Aethalometer filter to account for an increasing underestimation of the absorbance coefficient as the loading of the optically absorbing material on the filter increases. α_{ATN} is the specific absorption coefficient for ambient BC; the manufacturer's value of 16.6 $m^2\ g^{-1}$ is used in the UK national network. The symbols I'_0 and I' are used in their first appearance because these are not absolute values but calculated from changes in the light intensities over short periods of time (typically 5 min). The intensities I_0 and I are absolute intensities, describing the accumulated darkness of the spot rather than its change over a short time. A reflectance measurement of a PM sample is methodologically similar except that the light notionally passes twice rather than once through the sample. A correction for shadowing with increasing filter loading is likewise required,

and an analogous expression for the relationship between BC and R can be written,[24]

$$\mathrm{BC}(/\mu g\,m^{-3}) = K\ln\left(\frac{R_0}{R}\right)\left(1 + k'\ln\left(\frac{R_0}{R}\right)\right) \quad (2)$$

where the parameter K quantifies the relationship between BC and reflectance that is independent of the extent of filter loading (and includes within it α_{ATN} and values of A and V appropriate to Partisol sample collection), and the parameter k' quantifies the sensitivity of the underestimation of BC by reflectance as the filter darkness (strictly filter $\ln(R_0/R)$) increases. The values of k and k' in eqs 1 and 2 are not the same because of the different sampling geometries and wavelengths of light in the two techniques. Fitting eq 2 to a plot of Aethalometer BC against $\ln(R_0/R)$ for filters from colocated Partisol samples (Suppporting Information, Figure S1) gave values of $K = 1.8$ and $k' = 0.7$, which when substituted back into eq 2 yielded Partisol-reflectance-derived values of BC that regressed onto Aethalometer-derived values of BC with gradient 0.97, intercept 0.04, and $R^2 = 0.88$, i.e. a derivation of reflectance-derived BC values of high precision over the BC range 0−8 $\mu g\ m^{-3}$ encountered in this study. Equation 2 with the above values of K and k' was used to derive BC values from Partisol filter reflectance measurements at all sites, irrespective of whether an Aethalometer BC measurement was also available for a given sampling day at the urban background site. It is acknowledged that there is uncertainty in the application of this equation to PM_{10} samples collected at another site but similar uncertainty applies to the use of the single mass extinction coefficient of 16.6 $m^2\ g^{-1}$ to convert Aethalometer absorptions to BC concentrations at different locations.

The LOD for BC concentration, derived as the mean plus three times the SD of the BC values derived from reflectance measurements on all the Partisol machine-blank filters, was 0.02 $\mu g\ m^{-3}$. All sample BC concentrations exceeded this LOD.

Water-Soluble Organic Matter and Hydrophobic WSOM. Filters were sonicated for 30 min in 15 mL deionized water (18 MΩ), left to stand for a further 30 min, and the aqueous extract filtered through 0.22 μm syringe filters. Extracts were stored frozen until required.

Dissolved organic carbon (DOC) in the aqueous extracts was quantified with a Tekma-Dohrmann DC-80 total organic carbon analyzer using potassium hydrogen phthalate solutions as DOC standards. Sample DOC concentrations were corrected with the average of the DOC in the extracts from the two machine blank filters associated with each batch of two-week sample filters. Sample and blank filters from a two-week sampling batch were always extracted and analyzed in the same run. A factor 1.9 was applied to convert WSOC to WSOM based on the findings for PM by Kiss et al.[25] and Sun et al.[26] The LOD for the instrumental TOC determination was 0.22 mg L^{-1} which corresponds to an airborne WSOM concentration of 0.26 $\mu g\ m^{-3}$. Only 22 out of 730 determinations of WSOM were below this LOD; these data have been retained in the calculations of summary statistics. Sources of uncertainty not included in this analytical LOD include intersample uncertainty in the aqueous extraction from the PM and in the WSOM/WSOC scaling. Careful adherence to standardized field and laboratory procedures was used throughout. Relative uncertainties in WSOM of around 25% are likely realistic.

A subsequent separation of the WSOM was carried out to isolate the more hydrophobic components (HWSOM).[27] The aqueous extracts were acidified with 50 μL of 1 M phosphoric acid, loaded onto a methanol and phosphoric acid prewashed solid phase extraction (SPE) column (HyperSep C18, Thermo Fisher Scientific), and eluted with 2 × 2.5 mL LC-MS grade methanol. The combined eluate was evaporated to dryness (at ∼40 °C), the HWSOM was redissolved in 10 mL deionized water, and the solution freeze-dried over a period of 48 h. Any particularly volatile components of HWSOM may have been lost in this step. HWSOM is likely to be dominated by poly functional and poly conjugated material, for example, long-chained carboxylic acids and those containing aromatic rings, so is not anticipated to be particularly susceptible to loss in this procedure. Samples were subsequently stored frozen until required, when they were left to equilibrate for 1 h at ambient temperature and redissolved in 10 mL of deionized water for DOC determination as above. Initial trials showed there to be insufficient HWSOM per daily filter extract for accurate determination above an LOD so two-week batches of aqueous extracts were loaded onto a single SPE column. The HWSOM data therefore represent two-week averages, and the number of data are correspondingly considerably reduced. A UV−vis absorption spectrum in the wavelength range 240−500 nm was recorded for each HWSOM extract.

Raman Microscopy. A subset of filter samples (covering the range in PM_{10} masses and optical darkness) were analyzed with a Raman microscope (Renishaw inVia with WiRE 2.0 software) following the method of Ivleva et al.[19] Individual particles were illuminated at 514 nm (∼1 μm beam focus diameter) under ×50 magnification, and 8−10 spectra accumulated per particle over the range 800−2000 cm^{-1} (20−30 s integration time). Wavelength calibrations were performed using a silicon wafer and the first-order phonon band of Si at 520 cm^{-1}. Three single particles or particle agglomerates were selected at random on each of a subset of 18, 5, and 3 of the urban background, rural and roadside filters, respectively. Comparative Raman spectra were also acquired for samples of highly ordered pyrolytic graphite, urban particulate matter standard reference material (NIST SRM 1649a), a sample of exhaust PM scraped from the inside of the exhaust pipe of a diesel-engined service bus, and humic acid sodium salt (technical grade, Sigma-Aldrich). These materials were applied to the same type of quartz filters used for ambient sample collection.

A Raman spectrum of an ideal graphite lattice would contain a sharp peak around 1580 cm^{-1}, known as the G ("graphite") band.[28] The spectrum of disordered graphite contains another peak at around 1350 cm^{-1} known as the D ("defect") band, whose intensity increases relative to the G band as the graphitic structure becomes more disordered. A systematic investigation by Sadezky et al.[28] attributed the Raman spectra of soot particles to five different bands (G and D1−D4) and these band were subsequently used by Ivleva et al.[19] for the analysis of ambient particles. In this work, a five band spectrum of the G, D1, D2, D3, and D4 bands was fitted to each recorded Raman spectrum using a Gaussian line shape for the D3 band and a Lorentzian line shape for the remainder.[19,28,29] The smaller the D1 full-width half-maximum (fwhm) the greater the graphitic ordering of the associated carbon.

RESULTS AND DISCUSSION

Summary statistics for all measured components at each site are given in Table 1. Measurements were made for different durations at each site. Concurrent measurements at the urban background and roadside sites, and at the urban background and rural sites, were available for 209 and 48 days, respectively. Table 1 also provides the summary statistics restricted to each of these contemporaneous periods. There were insufficient samplers for measurements at all three sites simultaneously; hence while conclusions on relationships between particle metrics are valid on a pairwise site basis, caution is noted below when discussing comparative relationships across all three sites. It is possible that data from the shorter-duration sampling period at the rural site do not reflect the longer-term average characteristics at this site; but sampling here was for nearly two months, and southern Scotland does not have particularly strong seasonality in synoptic meteorology.

Black Carbon. Time series of the concentrations of BC at the three sites are shown in Supporting Information Figure S2. Average concentrations of BC at the three sites increased in the trend: rural < urban background < roadside (Table 1). Mean concentrations were 0.5, 1.2−1.6 and 3.4 μg m^{-3}, respectively. The range given for the urban background site reflects the variation in BC concentration obtained by averaging over the full data set at this site and for periods concurrent with measurements at the other sites (Table 1); the range of means for different averaging periods at the urban background site is considerably smaller than the spread of means across the sampling sites. These data are in line with measurements elsewhere in northern Europe. Viidanoja et al.[30] reported BC concentrations around 1.2 μg m^{-3} in Helsinki, Finland; and, similar to Edinburgh, Boogaard et al.[31] reported levels of BC in major streets in five cities in The Netherlands around twice those in the urban background.

The mean daily urban background increment (urban background−rural) in BC was 0.7 μg m^{-3} (n = 46) and is a measure of the amount, on average, of urban background BC that derives from sources within the city. It is about half of the mean urban background BC during this period. This proportion has declined from the inference almost a decade previously that approximately three-quarters of Edinburgh background BC (as quantified through the black smoke metric in that work) was local in origin.[32] This shows that with a decline in local BC sources the BC in regional background air has become relatively more important as a source of BC in the urban area.

The mean daily roadside increment (roadside−urban background) of 1.8 μg m^{-3} (n = 209) indicates the amount, on average, of BC at the roadside site that derives from adjacent traffic emissions of BC. Despite the important local traffic source of BC at the roadside site, the strong linear correlation between daily BC at the roadside and urban background sites (y = 2.21x − 0.15, r^2 = 0.82, n = 209; SI Table S1) shows that daily variations in BC concentration are generally controlled by common meteorological influences on dilution and dispersion.

The contribution of BC to PM_{10} varied with site type (Table 2). Mean daily contribution of BC to PM_{10} was 11% at the urban background site (BC:PM_{10} ratios were 11% or 9% when restricting comparisons to dates with simultaneous sampling at both background and roadside sites, or both background and rural sites, respectively), but the BC and PM_{10} were not well correlated (Table 2). This indicates some differences in

Table 2. Within-Site Daily Mean Ratios and Correlations for BC/PM_{10}, WSOM/PM_{10} and WSOM/BC

	urban background								roadside			rural		
	all data			data coincident with roadside			data coincident with rural							
	n	mean (SD)[a]	r^2	n	mean (SD)[a]	r^2	n	mean (SD)[a]	r^2	n	mean (SD)[a]	r^2	n	mean (SD)[a]	r^2
BC/PM_{10}	576	0.11 (0.06)	0.36	209	0.11 (0.05)	0.48	48	0.09 (0.10)	0.63	209	0.19 (0.075)	0.47	48	0.036 (0.020)	0.76
WSOM/PM_{10}	488	0.12 (0.08)	0.42	206	0.11 (0.08)	0.41	40	0.11 (0.08)	0.81	206	0.10 (0.04)	0.60	40	0.10 (0.05)	0.81
WSOM/BC	488	1.3 (0.9)	0.32	206	1.1 (0.7)	0.40	40	1.5 (0.6)	0.78	206	0.60 (0.34)	0.47	40	3.6 (2.2)	0.80

[a]SD = standard deviation.

dx.doi.org/10.1021/es500871k | Environ. Sci. Technol. 2014, 48, 8995−9003

influences on the two PM metrics. As BC is a fairly minor proportion of urban background PM_{10}, changes in BC do not greatly influence PM_{10}; for example, while BC concentrations are likely to be reduced by high wind speeds due to dilution, coarser components of PM_{10} increase due to resuspension. Venkatachari et al.[33] likewise noted that BC was of the order of 8−11% of $PM_{2.5}$, and variably correlated, for two sites in New York City. At the roadside site, BC contributed ∼19% on average to PM_{10}, consistent with the greater influence of locally derived traffic BC to PM_{10} at this location compared with the lower contribution of BC to PM_{10} in urban background air. A concentration wind-rose confirmed elevated BC from the directions of the adjacent roads at low windspeed. The correlation between BC and PM_{10} at the rural site was much stronger (r^2 = 0.76), showing that the rural site was generally sampling well-mixed background air. On average, BC contributed only ∼4% to PM_{10} during the period of sampling at the rural site.

BC was a major component of the roadside enhancement in PM_{10}. On average, for the 209 days of concurrent measurements, ∼60% of the roadside PM_{10} increment (mean: 2.8 μg m^{-3}) was accounted for by the roadside BC increment (mean: 1.8 μg m^{-3}), from which it can be inferred that ∼40% of the roadside PM_{10} increment derived from other exhaust emissions, that is, primary OM, and nonexhaust traffic sources such as brake and tire wear and resuspension of road dust. The ratio of primary OC to EC from traffic is subject to variability and uncertainty but recent analyses of measurement data suggests values in the range 0.3−0.4.[34] Applying a primary exhaust OM/OC scaling of ∼1.3,[35] and assuming equivalence of BC and EC concentrations, gives an estimate for traffic OM:BC ratio of ∼0.4−0.5, or an average contribution of primary OM at the Edinburgh roadside site of ∼0.7−0.9 μg m^{-3}. By subtraction, this yields an estimate of ∼0.3−0.5 μg m^{-3} for the contribution of other roadside sources to roadside PM_{10} at this location.

Water-Soluble Organic Matter. Time series of the concentrations of WSOM at the three sites are shown in Supporting Information Figure S3. The WSOM concentration of 10.8 μg m^{-3} derived for third January 2010 at the urban background site appears to be an analytical outlier. The concentration of PM_{10} was not elevated at this site on this day, nor were concentrations of WSOM elevated at the roadside site. Application of Grubbs' outlier test to the urban background WSOM data set provided evidence at $p < 0.01$ to reject this value. Following protocol reported in the UK Equivalence Programme for Monitoring of Particulate Matter,[36] application of Grubbs' test removed 3 further WSOM outlier data.

Average urban background, roadside and rural concentrations were 1.6−1.8, 1.8, and 1.6 μg m^{-3}, respectively (Table 1) where the range given for the urban background site reflects the variation in WSOM concentration obtained by averaging over the full data set at this site and for periods concurrent with measurements at the other sites. The average contribution of around 10% WSOM to PM_{10} at the background sites (Table 2) is broadly similar to the ∼8% contribution of WSOM to $PM_{2.5}$ reported for a coastal site in Portugal.[37] The similar concentrations of WSOM at all three sites implies a common background WSOM component, in contrast to BC whose average concentration at roadside was a factor 2 and 7 times greater than at the urban background and rural sites, respectively, indicating local urban sources. The very strong correlations between daily WSOM at the roadside and urban background sites (r^2 = 0.90, regression gradient 1.04, n = 201) and at the rural and urban background sites (r^2 = 0.90, regression gradient 0.89, n = 39; SI Table S1), albeit for separate data collection periods, are also consistent with a geographically homogeneous contribution of PM_{10} WSOM.

Daily WSOM and BC were strongly correlated at the rural site (r^2 = 0.80, n = 40) (Table 2), again consistent with the dominance of a regional background for both these components at this site whose concentration variations are determined by meteorology rather than by local sources. In fact, correlations between PM_{10}, BC and WSOM were all substantially higher at the rural site than the other sites showing that the rural site was in general sampling well-mixed background air. The rural background concentrations of WSOM were, on average, 2.9 times greater than rural BC concentrations. In contrast, at the roadside site correlation between WSOM and BC was weaker (r^2 = 0.46, n = 202, although for a different time period of sampling c.f. the rural data set), with daily BC concentrations a factor 2.3 times greater than WSOM concentrations, on average. Concentration wind-roses indicated elevated WSOM at low wind speeds and for wind directions from the southeast. This indicates the influence of long-range transport of OM from continental sources. Significantly enhanced total OC and secondary OC in $PM_{2.5}$ from easterly and southerly air-mass back trajectories has similarly been reported for measurements in Birmingham, UK.[5] Overall, the observations are consistent with the slow transformation of emitted OM into WSOM on a background spatial scale.[38]

Despite the dominance of the background component to WSOM, there is evidence for a small roadside increment in WSOM of ∼0.12 μg m^{-3} (the average daily increment for concurrent measurements), whose source must be traffic-related OM. Analyses described at the end of the "Black Carbon" results section above suggest the traffic-related OM component comprises ∼0.7−0.9 μg m^{-3}. The data from the aqueous extractions therefore indicate that only ∼15% of this traffic-derived OM is water-soluble (assuming that none of the material characterized as BC is water-soluble). This is consistent with the view that fresh exhaust primary OM comprises predominantly nonpolar, nonfunctionalized hydrocarbons. Instead, the traffic-related WSOM component may well be nonexhaust in origin. A traffic-related "resuspension" OM particle source could include fragments of primary biological material (plant, pollen, spores, etc.), that is, compounds such as amino acids, carbohydrates, and cellulose, and also soluble humic acid from suspended soil particles. The broader implication is the indirect evidence in support of a nonexhaust traffic-related "resuspension" source of particles in the urban environment.

Hydrophobic WSOM. On average, ∼30% of the WSOM extracted from PM_{10} was subsequently isolated via SPE as "hydrophobic WSOM". The HWSOM concentrations are summarized in Table 1. The average relative roadside increment in HWSOM (∼16%) is significantly greater than the relative roadside increment in WSOM (∼8%), showing that traffic-derived WSOM (albeit small in absolute concentration) is more hydrophobic in nature than the more aged general urban background WSOM, as reported also by Salma et al.[39]

UV−vis Characterization of HWSOM. The UV−vis spectra of the bulked dissolved HWSOM samples were generally featureless curves with increasing absorption to shorter wavelength in the range 500−240 nm. The general

similarity of UV−vis spectra of water-soluble OM extracted from atmospheric PM with those for terrestrial and aquatic humic acids has led to the former substances being termed humic-like substances (HULIS),[40] although it has also been argued that this is not an appropriate descriptor.[41]

Figure 1 shows the absorbance at 250 nm plotted against HWSOM concentration for samples collected at the urban

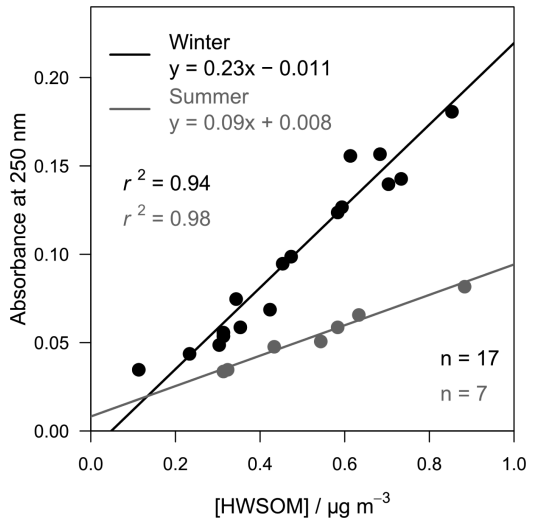

Figure 1. Absorbance at 250 nm versus HWSOM concentration for samples collected at the urban background site during winter (November−February) and summer (May−August).

background site in summer (defined here as May−August) and in winter (defined as November−February). Correlations were very high in both seasons (r^2 = 0.94 and 0.98 for winter and summer, respectively) but the distinct gradients in each case indicate seasonal differences in the chemical structures of the absorbers arising from seasonal differences in sources and/or atmospheric transformation processes.

To eliminate concentration effects, time series of the specific absorbances (mgC^{-1} m^3 cm^{-1}) at 250 nm for HWSOM samples from the three sites are plotted in Figure 2. Specific absorbances are significantly lower in the summer than in the winter. This implies increased prevalence of C═C and C═O unsaturated bonds in the HWSOM in winter (compared with

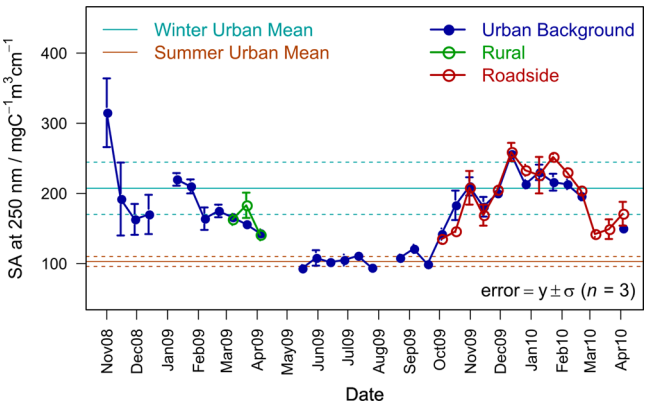

Figure 2. Time series of specific absorbance at 250 nm for HWSOM samples from the urban background, roadside and rural sites. The horizontal lines show the winter and summer means and the associated dashed lines are the standard deviations from the mean.

summer), as observed also for urban background France.[42] The lower temperatures in winter increase the partitioning of lower volatility VOC emissions into the particle phase. The partitioning of species between gas and condensed phase is a strong function of temperature through the vapor pressure of the species at a given temperature. The vapor pressure is in turn dependent on the molecular structure. Unsaturated bonds, particularly the heteronuclear unsaturated bond C═O (and other heteronuclear bonds), increases the dipole of the species and decreases its vapor pressure at a given temperature. For less-volatile species which partition in significant amounts to both phases the change in partitioning with the change in ambient temperature becomes materially relevant.

A useful diagnostic from these UV−vis spectra is the ratio of absorbances at different wavelengths. For aquatic humic substances, Peuravuori and Pihlaja[43] showed that the quotient E_2/E_3 (absorbances at 250 and 365 nm, respectively) had a strong inverse correlation with the total aromaticity and averaged molecular weights of all the humic solutes they analyzed. Figure 3 shows the time series of this quotient for the

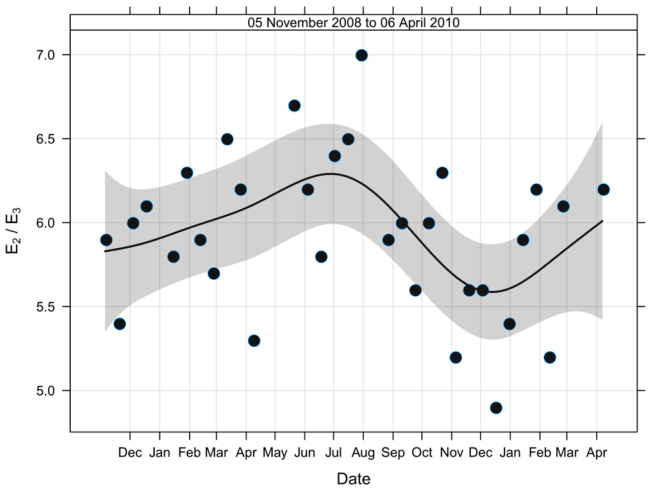

Figure 3. Time series of E_2/E_3 ratio for HWSOM samples from the urban background site. The smoothed trend line is a spline (with 95% confidence intervals shaded in gray) calculated using a general additive model in R.[50]

samples of HWSOM from the urban background samples in this work. The E_2/E_3 ratio has a summer maximum (proportionally lower conjugation/aromaticity) and a winter minimum (proportionally greater conjugation/aromaticity). The same pattern was observed in rural Portugal,[21] urban background France[42] and urban New Zealand.[44] The implication of increased aromaticity in the OM in winter has been attributed by some workers to increased wood burning in this season;[45,46] but evidence presented above indicates that the majority of WSOM and HWSOM measured at the urban background site in this work is associated with a regional background, so this seasonality in E_2/E_3 ratio likely reflects seasonality in the regional HWSOM brought to Edinburgh via long-range transport (rather than local wood burning sources). The annual mean values for the UV absorption component from the AE22 Aethalometer at the urban background site is the smallest of all the AE22 Aethalometers in urban locations in the UK national network,[47] which is consistent with the interpretation that contribution of local wood burning to carbonaceous PM in Edinburgh is small. It also seems likely

dx.doi.org/10.1021/es500871k | Environ. Sci. Technol. 2014, 48, 8995−9003

that the lower temperatures in winter lead to relatively greater partitioning of the more aromatic components of the low volatility organic compounds into the particle phase. Secondary formation processes that dominate in the summer tend to yield particulate OM with more aliphatic nonconjugated character.[48] Primary production of biogenic HWSOM over the North Atlantic could also be a summertime contributor to oxidized species with extended aliphatic moieties.[49]

Raman Microspectroscopy of Individual Particles. The Raman bands with largest intensity and peak separations are the G band (initial position 1580 cm^{-1}) and the D1 band (initial position 1360 cm^{-1}). The smaller the D1 fwhm value the greater the graphitic ordering of the associated carbon. The fwhm values for the D1 band obtained from the curve fittings for the highly ordered pyrolytic graphite, diesel exhaust, SRM 1649a and humic acid samples analyzed were, respectively, 37 ± 2 cm^{-1}, 142 ± 10 cm^{-1}, 200 ± 48 cm^{-1}, and 230 ± 38 cm^{-1} (SD of triplicates), consistent with the inverse correlation between D1 fwhm and proportion of EC reported previously.[19] The Raman method demonstrates clear discrimination in type of carbon, and shows that diesel exhaust is not simply graphitic soot but has spectral features indicating more functionalized carbon. The Raman data show humic acid to be more functionalized still.

Figure 4 plots the mean D1 fwhm value for each daily sample analyzed against the corresponding BC concentration. The D1

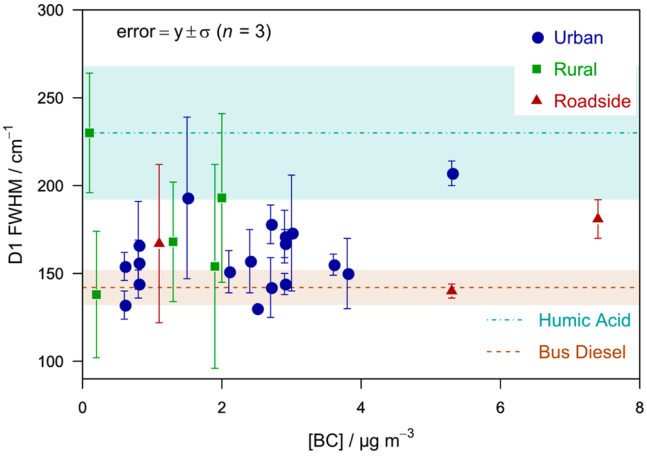

Figure 4. Raman D1 fwhm values (mean ±1 SD for three particles per filter) against BC concentrations for a subset of PM_{10} samples from the three sites. Also shown are mean D1 fwhm values for the diesel bus exhaust and humic acid materials, with bands of shading indicating their ±1 SD ranges.

fwhm values for the samples of diesel exhaust and humic acid material are also illustrated. For many filter samples there was large standard deviation in D1 fwhm values across the three particles selected for analysis. This was particularly the case for spectra acquired from particles in rural samples and can be attributed to heterogeneity between individual particles in a sample. The number of Raman spectra acquired per filter was a compromise between obtaining replicate statistics per filter and analyses of a spread in sample filters. Nevertheless, Figure 4 shows that the D1 fwhm values of nearly all PM_{10} samples analyzed are within the range demarcated by the diesel exhaust and humic acid samples, and all are within the 1 SD uncertainty ranges for these materials. There is no discernible relationship between D1 fwhm and BC concentration, although it is notable that he highest D1 fwhm value at the urban background site corresponds with the highest urban background BC concentration. This sample was collected on 5th November 2009—5th November is Guy Fawkes Night in the UK which is traditionally celebrated with bonfires and fireworks—and the D1 fwhm value indicates a high degree of complex carbonaceous material, presumably from the bonfires, rather than the more graphitic-like soot associated with diesel emissions. In general, however, the urban sample fwhm values indicate the presence of both exhaust-like carbonaceous material and more functionalized carbon. The mean (±1 standard error) D1 fwhm values for samples from the urban background, rural, and roadside locations were 159 ± 5 cm^{-1} (n = 18), 177 ± 16 cm^{-1} (n = 5), and 163 ± 12 cm^{-1} (n = 3), respectively. Although these data are based on limited measurements, there is a tendency toward more humic-like D1 fwhm values for the rural samples, on average, compared with the urban samples.

Results overall indicate presence of a background functionalized carbonaceous organic material, with local graphitic-like BC sources superimposed. The influence of roadside-related BC appears to be substantially dispersed in urban background air. It is anticipated that these findings in Edinburgh are broadly representative for cities and large towns in northern Europe, although actual roadside-urban background increments at a given location will depend on local traffic count and urban meteorology. In general, however, mitigation of exhaust and nonexhaust PM emissions will directly act on near-roadside concentrations but also on the component of background OM derived ultimately from emitted carbonaceous material regionally.

■ ASSOCIATED CONTENT

Ⓢ Supporting Information

Plot of Aethalometer BC against Partisol filter $\ln(R_0/R)$ at the urban background site (Figure S1), and time series of daily BC and WSOM concentrations (Figures S2 and S3) at the urban background, roadside and rural sites. Correlations and linear regressions of each PM component between sites (Table S1). This material is available free of charge via the Internet at http://pubs.acs.org/.

■ AUTHOR INFORMATION

Corresponding Author

*Phone: 0131 6504764; fax: 0131 6506453; e-mail: m.heal@ed.ac.uk.

Notes

The authors declare no competing financial interest.

■ ACKNOWLEDGMENTS

M.D.H. gratefully acknowledges PhD studentship funding from the UK Natural Environment Research Council (NERC). We thank colleagues from the City of Edinburgh Council, the University of Edinburgh and the NERC Centre for Ecology & Hydrology for permission to site PM samplers at the urban background, roadside and rural sites, respectively. We also thank John Parker (Scottish Agricultural College) for access to the DOC analyser, and Andrei Gromov (University of Edinburgh) for guidance with Raman analyses. We thank the reviewers of this paper who contributed many helpful comments for its improvement.

REFERENCES

(1) Heal, M. R.; Kumar, P.; Harrison, R. M. Particles, air quality, policy and health. *Chem. Soc. Rev.* **2012**, *41*, 6606−6630.

(2) AQEG Particulate Matter in the United Kingdom. Second report of the Air Quality Expert Group. 2005, UK Department for Environment, Food and Rural Affairs, PB10580, London. http://www.defra.gov.uk/environment/quality/air/air-quality/committees/aqeg/publish/.

(3) USEPA Integrated Science Assessment for Particulate Matter. *EPA/600/R-08/139F*; United States Environmental Protection Agency, 2009, http://cfpub.epa.gov/ncea/cfm/recordisplay.cfm?deid=216546.

(4) Harrison, R. M.; Yin, J. X. Sources and processes affecting carbonaceous aerosol in central England. *Atmos. Environ.* **2008**, *42*, 1413−1423.

(5) Heal, M. R.; Naysmith, P.; Cook, G. T.; Xu, S.; Raventos Duran, T.; Harrison, R. M. Application of ^{14}C analyses to source apportionment of carbonaceous $PM_{2.5}$ in the UK. *Atmos. Environ.* **2011**, *45*, 2341−2348.

(6) Putaud, J.; Van Dingenen, R.; Alastuey, A.; Bauer, H.; Birmili, W.; Cyrys, J.; Flentje, H.; Fuzzi, S.; Gehrig, R.; et al. A European aerosol phenomenology-3: Physical and chemical characteristics of particulate matter from 60 rural, urban, and kerbside sites across Europe. *Atmos. Environ.* **2010**, *44*, 1308−1320.

(7) Yin, J. X.; Harrison, R. M. Pragmatic mass closure study for $PM_{1.0}$, $PM_{2.5}$ and PM_{10} at roadside, urban background and rural sites. *Atmos. Environ.* **2008**, *42*, 980−988.

(8) Fuzzi, S.; Andreae, M. O.; Huebert, B. J.; Kulmala, M.; Bond, T. C.; Boy, M.; Doherty, S. J.; Guenther, A.; Kanakidou, M.; et al. Critical assessment of the current state of scientific knowledge, terminology, and research needs concerning the role of organic aerosols in the atmosphere, climate, and global change. *Atmos. Chem. Phys.* **2006**, *6*, 2017−2038.

(9) Hallquist, M.; Wenger, J. C.; Baltensperger, U.; Rudich, Y.; Simpson, D.; Claeys, M.; Dommen, J.; Donahue, N. M.; George, C.; et al. The formation, properties and impact of secondary organic aerosol: Current and emerging issues. *Atmos. Chem. Phys.* **2009**, *9*, 5155−5235.

(10) Harrison, R. M.; Jones, A. M.; Gietl, J.; Yin, J.; Green, D. C. Estimation of the contributions of brake dust, tire wear, and resuspension to nonexhaust traffic particles derived from atmospheric measurements. *Environ. Sci. Technol.* **2012**, *46*, 6523−6529.

(11) Yin, J.; Harrison, R. M.; Chen, Q.; Rutter, A.; Schauer, J. J. Source apportionment of fine particles at urban background and rural sites in the UK atmosphere. *Atmos. Environ.* **2010**, *44*, 841−851.

(12) Charron, A.; Harrison, R. M. Fine ($PM_{2.5}$) and coarse ($PM_{2.5-10}$) particulate matter on a heavily trafficked London highway: Sources and processes. *Environ. Sci. Technol.* **2005**, *39*, 7768−7776.

(13) Perez, N.; Pey, J.; Cusack, M.; Reche, C.; Querol, X.; Alastuey, A.; Viana, M. Variability of particle number, black carbon, and PM_{10}, $PM_{2.5}$, and PM_1 levels and speciation: Influence of road traffic emissions on urban air quality. *Aerosol Sci. Technol.* **2010**, *44*, 487−499.

(14) Peltier, R. E.; Cromar, K. R.; Ma, Y.; Fan, Z. H.; Lippmann, M. Spatial and seasonal distribution of aerosol chemical components in New York City: (2) Road dust and other tracers of traffic-generated air pollution. *J. Expos. Sci. Environ. Epidemiol.* **2011**, *21*, 484−494.

(15) Pant, P.; Harrison, R. M. Estimation of the contribution of road traffic emissions to particulate matter concentrations from field measurements: A review. *Atmos. Environ.* **2013**, *77*, 78−97.

(16) Cyrys, J.; Heinrich, J.; Hoek, G.; Meliefste, K.; Lewne, M.; Gehring, U.; Bellander, T.; Fischer, P.; Van Vliet, P.; et al. Comparison between different traffic-related particle indicators: Elemental. carbon (EC), $PM_{2.5}$ mass, and absorbance. *J. Expos. Sci. Environ. Epidemiol.* **2003**, *13*, 134−143.

(17) Reche, C.; Querol, X.; Alastuey, A.; Viana, M.; Pey, J.; Moreno, T.; Rodriguez, S.; Gonzalez, Y.; Fernandez-Camacho, R.; et al. New considerations for PM, black carbon and particle number concentration for air quality monitoring across different European cities. *Atmos. Chem. Phys.* **2011**, *11*, 6207−6227.

(18) Mertes, S.; Dippel, B.; Schwarzenbock, A. Quantification of graphitic carbon in atmospheric aerosol particles by Raman spectroscopy and first application for the determination of mass absorption efficiencies. *J. Aerosol Sci.* **2004**, *35*, 347−361.

(19) Ivleva, N. P.; McKeon, U.; Niessner, R.; Poschl, U. Raman microspectroscopic analysis of size-resolved atmospheric aerosol particle samples collected with an ELPI: Soot, humic-like substances, and inorganic compounds. *Aerosol Sci. Technol.* **2007**, *41*, 655−671.

(20) Deboudt, K.; Flament, P.; Choel, M.; Gloter, A.; Sobanska, S.; Colliex, C. Mixing state of aerosols and direct observation of carbonaceous and marine coatings on African dust by individual particle analysis. *J. Geophys. Res.* **2010**, *115*, D24207 DOI: 10.1029/2010JD013921.

(21) Duarte, R. M. B. O.; Pio, C. A.; Duarte, A. C. Spectroscopic study of the water-soluble organic matter isolated from atmospheric aerosols collected under different atmospheric conditions. *Anal. Chim. Acta* **2005**, *530*, 7−14.

(22) *CEN Air Quality—Determination of the PM10 Fraction of Suspended Particulate Matter - Reference Method and Field Test Procedure to Demonstrate Reference Equivalence of Measurement Methods*, EN 12341:1998; European Committee for Standardisation (CEN), 1998.

(23) Virkkula, A.; Makela, T.; Hillamo, R.; Yli-Tuomi, T.; Hirsikko, A.; Hameri, K.; Koponen, I. K. A simple procedure for correcting loading effects of aethalometer data. *J. Air Waste Manage. Assoc.* **2007**, *57*, 1214−1222.

(24) Heal, M. R.; Quincey, P. The relationship between black carbon concentration and black smoke: A more general approach. *Atmos. Environ.* **2012**, *54*, 538−544.

(25) Kiss, G.; Varga, B.; Galambos, I.; Ganszky, I. Characterization of water-soluble organic matter isolated from atmospheric fine aerosol. *J. Geophys. Res.* **2002**, *107*, 8339 DOI: 10.1029/2001JD000603.

(26) Sun, Y.; Zhang, Q.; Zheng, M.; Ding, X.; Edgerton, E. S.; Wang, X. Characterization and source apportionment of water-soluble organic matter in atmospheric fine particles ($PM_{2.5}$) with high-resolution aerosol mass spectrometry and GC-MS. *Environ. Sci. Technol.* **2011**, *45*, 4854−4861.

(27) Varga, B.; Kiss, G.; Ganszky, I.; Gelencser, A.; Krivacsy, Z. Isolation of water-soluble organic matter from atmospheric aerosol. *Talanta* **2001**, *55*, 561−572.

(28) Sadezky, A.; Muckenhuber, H.; Grothe, H.; Niessner, R.; Poschl, U. Raman micro spectroscopy of soot and related carbonaceous materials: Spectral analysis and structural information. *Carbon* **2005**, *43*, 1731−1742.

(29) Ivleva, N. P.; Messerer, A.; Yang, X.; Niessner, R.; Poschl, U. Raman microspectroscopic analysis of changes in the chemical structure and reactivity of soot in a diesel exhaust aftertreatment model system. *Environ. Sci. Technol.* **2007**, *41*, 3702−3707.

(30) Viidanoja, J.; Sillanpaa, M.; Laakia, J.; Kerminen, V. M.; Hillamo, R.; Aarnio, P.; Koskentalo, T. Organic and black carbon in PM2.5 and PM10:1 year of data from an urban site in Helsinki, Finland. *Atmos. Environ.* **2002**, *36*, 3183−3193.

(31) Boogaard, H.; Kos, G. P. A.; Weijers, E. P.; Janssen, N. A. H.; Fischer, P. H.; Van der Zee, S. C.; de Hartog, J. J.; Hoek, G. Contrast in air pollution components between major streets and background locations: Particulate matter mass, black carbon, elemental composition, nitrogen oxide and ultrafine particle number. *Atmos. Environ.* **2011**, *45*, 650−658.

(32) Heal, M. R.; Hibbs, L. R.; Agius, R. M.; Beverland, I. J. Interpretation of variations in fine, coarse and black smoke particulate matter concentrations in a Northern European city. *Atmos. Environ.* **2005**, *39*, 3711−3718.

(33) Venkatachari, P.; Zhou, L. M.; Hopke, P. K.; Felton, D.; Rattigan, O. V.; Schwab, J. J.; Demerjian, K. L. Spatial and temporal variability of black carbon in New York City. *J. Geophys. Res.* **2006**, *111*, D10S05 DOI: 10.1029/2005JD006314.

(34) Pio, C.; Cerqueira, M.; Harrison, R. M.; Nunes, T.; Mirante, F.; Alves, C.; Oliveira, C.; Sanchez de la Campa, A.; Artíñano, B.; et al. OC/EC ratio observations in Europe: Re-thinking the approach for

apportionment between primary and secondary organic carbon. *Atmos. Environ.* **2011**, *45*, 6121−6132.
(35) AQEG Fine Particulate Matter (PM2.5) in the United Kingdom. Air Quality Expert Group. 2012, UK Department for Environment, Food and Rural Affairs, London. PB138379. http://uk-air.defra.gov.uk/library/reports?report_id=727.
(36) Harrison, D. UK equivalence programme for monitoring of particulate matter. *Bureau Veritas report for Defra*. **2006**, *BV/AQ/AD202209/DH/2396*, http://www.airquality.co.uk/archive/reports/cat05/0606130952_UKPMEquivalence.pdf.
(37) Duarte, R. M. B. O.; Santos, E. B. H.; Pio, C. A.; Duarte, A. C. Comparison of structural features of water-soluble organic matter from atmospheric aerosols with those of aquatic humic substances. *Atmos. Environ.* **2007**, *41*, 8100−8113.
(38) Jimenez, J.; Canagaratna, M.; Donahue, N.; Prevot, A.; Zhang, Q.; Kroll, J.; DeCarlo, P.; Allan, J.; Coe, H.; et al. Evolution of organic aerosols in the atmosphere. *Science* **2009**, *326*, 1525−1529.
(39) Salma, I.; Ocskay, R.; Chi, X.; Maenhaut, W. Sampling artefacts, concentration and chemical composition of fine water-soluble organic carbon and humic-like substances in a continental urban atmospheric environment. *Atmos. Environ.* **2007**, *41*, 4106−4118.
(40) Havers, N.; Burba, P.; Lambert, J.; Klockow, D. Spectroscopic characterization of humic-like substances in airborne particulate matter. *J. Atmos. Chem.* **1998**, *29*, 45−54.
(41) Graber, E. R.; Rudich, Y. Atmospheric HULIS: How humic-like are they? A comprehensive and critical review. *Atmos. Chem. Phys.* **2006**, *6*, 729−753.
(42) Baduel, C.; Voisin, D.; Jaffrezo, J. Seasonal variations of concentrations and optical properties of water soluble HULIS collected in urban environments. *Atmos. Chem. Phys.* **2010**, *10*, 4085−4095.
(43) Peuravuori, J.; Pihlaja, K. Molecular size distribution and spectroscopic properties of aquatic humic substances. *Anal. Chim. Acta* **1997**, *337*, 133−149.
(44) Krivacsy, Z.; Kiss, G.; Ceburnis, D.; Jennings, G.; Maenhaut, W.; Salma, I.; Shooter, D. Study of water-soluble atmospheric humic matter in urban and marine environments. *Atmos. Res.* **2008**, *87*, 1−12.
(45) Favez, O.; Cachier, H.; Sciare, J.; Sarda-Esteve, R.; Martinon, L. Evidence for a significant contribution of wood burning aerosols to $PM_{2.5}$ during the winter season in Paris, France. *Atmos. Environ.* **2009**, *43*, 3640−3644.
(46) Fuller, G. W.; Sciare, J.; Lutz, M.; Moukhtar, S.; Wagener, S. New Directions: Time to tackle urban wood burning? *Atmos. Environ.* **2013**, *68*, 295−296.
(47) Butterfield, D. M.; Beccaceci, S.; Sweeney, B.; Williams, M.; Fuller, G.; Green, D.; Grieve, A. *2010 Annual Report for the UK Black Carbon Network*, NPL Report AS 63; National Physics Laboratory: Teddington, UK, 2011; http://publications.npl.co.uk/npl_web/pdf/as63.pdf.
(48) Samburova, V.; Szidat, S.; Hueglin, C.; Fisseha, R.; Baltensperger, U.; Zenobi, R.; Kalberer, M. Seasonal variation of high-molecular-weight compounds in the water-soluble fraction of organic urban aerosols. *J. Geophys. Res.* **2005**, *110*, D23210 DOI: 10.1029/2005JD005910.
(49) O'Dowd, C. D.; Facchini, M. C.; Cavalli, F.; Ceburnis, D.; Mircea, M.; Decesari, S.; Fuzzi, S.; Yoon, Y. J.; Putaud, J. P. Biogenically driven organic contribution to marine aerosol. *Nature* **2004**, *431*, 676−680.
(50) Carslaw, D. C.; Ropkins, K. openair - An R package for air quality data analysis. *Environ. Modell. Software* **2012**, *27−28*, 52−61.